

# Constraints on sterile neutrinos as dark matter candidates from the diffuse X-ray background

A. Boyarsky,<sup>1,2★</sup> A. Neronov,<sup>3,4†</sup> O. Ruchayskiy<sup>5</sup> and M. Shaposhnikov<sup>1,2</sup>

<sup>1</sup>CERN, Theory department, CH-1211 Geneva 23, Switzerland

<sup>2</sup>École Polytechnique Fédérale de Lausanne, Institute of Theoretical Physics, FSB/ITP/LPPC, BSP 720, CH-1015, Lausanne, Switzerland

<sup>3</sup>INTEGRAL Science Data Centre, Chemin d'Écogia 16, 1290 Versoix, Switzerland

<sup>4</sup>Geneva Observatory, 51 ch. des Maillettes, CH-1290 Sauverny, Switzerland

<sup>5</sup>Institut des Hautes Études Scientifiques, Bures-sur-Yvette, F-91440, France

Accepted 2006 April 15. Received 2006 April 5; in original form 2006 January 10

## ABSTRACT

Sterile neutrinos with masses in the kilo-electronvolt range are viable candidates for the warm dark matter. We analyse existing data for the extragalactic diffuse X-ray background for signatures of sterile neutrino decay. The absence of a detectable signal within current uncertainties of background measurements puts model-independent constraints on allowed values of the sterile neutrino mass and mixing angle, which we present in this work.

**Key words:** neutrinos – dark matter – X-rays: diffuse background.

## 1 INTRODUCTION

At the present time there exists an extensive body of evidence that most of the matter in the Universe is composed of new, as yet undiscovered particles – the dark matter (DM). Observations of (i) galactic rotation curves, (ii) cosmic microwave background radiation, (iii) gravitational lensing, and (iv) X-ray emission of hot gas in clusters of galaxies provide independent measurements of the DM content of the Universe.

A further major experimental discovery of the last decade is that of neutrino oscillations. There are separate measurements of neutrino oscillations in solar neutrinos (Ahmad et al. 2002), atmospheric neutrinos (Fukuda et al. 1998), and reactor neutrinos (Eguchi et al. 2003). Neutrino oscillations can be explained if a neutrino is a massive particle, which is contrary to the Standard Model assumption. This means that, along with the usual left-handed (or *active*) neutrinos, there may also exist right-handed (or *sterile*) neutrinos.

The conventional see-saw mechanism (Minkowski 1977; Yanagida 1979, 1980; Gell-Mann, Ramond & Slansky 1980; Ramond 1979; Mohapatra & Senjanovic 1980; Glashow 1980) for the generation of small active neutrino masses implies that the sterile neutrinos are heavy (usually of the order of the grand unification theory (GUT) energy scale,  $\sim 10^{10}$ – $10^{15}$  GeV) and that their mixing with usual matter is of the order of  $\sin \theta \sim 10^{-10}$ – $10^{-15}$ . In addition to the smallness of neutrino masses, models of this type can explain the baryon asymmetry of the Universe via thermal leptogenesis (Fukugita & Yanagida 1986) and anomalous electroweak

fermion number non-conservation (Kuzmin, Rubakov & Shaposhnikov 1985). They do not, however, offer a DM candidate.

Recently it was proposed that neutrino oscillations, the origin of the dark matter, and the baryon asymmetry of the Universe could be consistently explained in a model termed the ‘neutrino Minimal Standard Model’ ( $\nu$ MSM) (Asaka, Blanchet & Shaposhnikov 2005; Asaka & Shaposhnikov 2005). This model is a natural extension of the Minimal Standard Model (MSM), in which three right-handed neutrinos are introduced into the MSM Lagrangian. In this extension, neutrinos obtain Dirac masses via Yukawa coupling analogous to the other quarks and leptons of the MSM, and in addition Majorana mass terms are allowed for right-handed neutrinos. Unlike conventional see-saw scenarios, all of these Majorana masses (which are roughly equal to the masses of corresponding sterile neutrinos) are chosen such that the mass of the lightest sterile neutrino is in the kilo-electronvolt range, and the others are  $\lesssim 100$  GeV – below the electroweak symmetry-breaking scale. In this model, the role of the dark matter particle is played by the lightest sterile neutrino.

The existence of a relatively light sterile neutrino has non-trivial observable consequences for cosmology and astrophysics. It was proposed in Dodelson & Widrow (1993) that a sterile neutrino with a mass in the kilo-electronvolt range may be a viable ‘warm’ DM candidate. The small mixing angle ( $\sin \theta \sim 10^{-6}$ – $10^{-4}$ ) between sterile and active neutrinos ensures that sterile neutrinos were never in thermal equilibrium in the early Universe and thus allows their abundance to be smaller than the equilibrium one. Moreover, a sterile neutrino with these parameters is important for the physics of supernovas (Fryer & Kusenko 2006), and was proposed as an explanation of the pulsar kick velocities (Kusenko & Segre 1997; Fuller et al. 2003; Barkovich, D’Olivo & Montemayor 2004).

In addition to the dominant decay mode into three active neutrinos, the light (with mass  $m_s \lesssim 1$  MeV) sterile neutrino can decay into an active one and a photon with energy  $E_\gamma = m_s/2$ . Thus, there

★On leave of absence from Bogolyubov Institute of Theoretical Physics, Kyiv, Ukraine.

†E-mail: andrii.neronov@obs.unige.ch

exists a possibility of direct detection of neutrino-decay emission lines from sources with a high concentration of DM, for example from clusters of galaxies (Abazajian et al. 2001). Similarly, the signal from radiative sterile neutrino decays accumulated over the history of the Universe could be seen as a feature in the diffuse extragalactic background light spectrum. This opens up the possibility of studying the physics beyond the Standard Model using astrophysical observations.

Recently there have been a number of works devoted to the analysis of the possibility of discovering sterile neutrino radiative decay from X-ray observations (Abazajian et al. 2001; Mapelli & Ferrara 2005). For example, it was argued by Abazajian et al. (2001) that, if sterile neutrinos made up 100 per cent of all the DM, one should be able to detect the DM decay line against the background of the X-ray emission from the Virgo cluster. According to Abazajian et al. (2001), the non-detection of the line puts an upper limit of  $m_s < 5$  keV on the neutrino mass [this limit was, however, recently revised in Abazajian (2006), who finds the restriction  $m_s < 8$  keV]. It was also noted by Abazajian et al. (2001) and Mapelli & Ferrara (2005) that one can obtain even stronger constraints,  $m_s \lesssim 2$  keV, from the diffuse extragalactic X-ray background (XRB) under the assumption that the dark matter in the Universe is uniformly distributed up to distances corresponding to redshifts  $z \ll 1$ . Together with the claims of Hansen et al. (2002) and Viel et al. (2005), putting a lower bound of  $m_s > 2$  keV on the neutrino mass from Lyman  $\alpha$  forest observations, this would lead to a very narrow window for allowed sterile neutrino masses, if not excluding it completely.

In this paper we re-analyse the limit imposed on the parameters of sterile neutrinos from the observations of the diffuse XRB. In order to do this, we process actual astrophysical data from *HEAO-1* and *XMM-Newton* missions. There are several motivations for this.

(i) All the above restrictions on sterile neutrino mass (Abazajian et al. 2001; Dolgov & Hansen 2002; Mapelli & Ferrara 2005; Abazajian 2006) are model-dependent and based on the assumption that sterile neutrinos were absent in the early Universe at temperatures greater than a few giga-electronvolts. Depending on the model, the relationship between the mass of sterile neutrino, the mixing angle and the present-day sterile neutrino density,  $\Omega_s$ , changes. In fact, to compute the sterile neutrino abundance one needs to know whether there was any substantial lepton asymmetry of the Universe at the time of sterile neutrino production, what the coupling of sterile neutrinos to other particles such as inflatons or supersymmetric particles is, etc.<sup>1</sup> Moreover, even if these uncertainties were removed, a reliable computation of the relic abundance of sterile neutrinos is very difficult as the peak of their production falls on the Quantum Chromodynamics (QCD) epoch of the Universe evolution, corresponding to the temperature  $\sim 150$  MeV (Dodelson & Widrow 1993), where neither a quark–gluon nor hadronic description of the plasma is possible. Therefore, until the particle physics model is fully specified and the physics of a hadronic plasma is fully understood, one cannot put a robust restriction on one single parameter, such as  $m_s$ , of the model.

Therefore we aim in this paper at a clear separation between the model-independent predictions, based solely on astrophysical observations, and any statements that depend on a given model and underlying assumptions. To this end, we treat  $m_s$  and  $\sin \theta$  as two

independent parameters, and present the limits in the form of an ‘exclusion plot’ in the  $(m_s; \Omega_s \sin^2 2\theta)$  parameter space.

It should be stressed that our data analysis is not based on any specific model of sterile neutrinos, and as such can be applied to any ‘warm’ DM candidate particle that has a radiative decay channel. In the case of sterile neutrinos, the full decay width of this process is related to the parameter  $\sin \theta$  via equation (4) (see below).

(ii) In contrast to previous works (Abazajian et al. 2001; Mapelli & Ferrara 2005), we argue that the non-isotropy or ‘clumpiness’ of the matter distribution in the nearby Universe *does not* relax the limit on the neutrino mass. Indeed, the fact that a significant part of the dark matter at redshifts  $z \lesssim 10$  is concentrated in galaxies and clusters of galaxies just means that the strongest signal from the dark matter decay should come from the sum of the signals from the compact sources at  $z \lesssim 10$ . Taking into account that the DM decay signal from  $z \lesssim 10$  is some two orders of magnitude stronger than that from  $z \gtrsim 10$ , while the subtraction of resolved sources reduces the residual X-ray background maximum by a factor of 10, we argue that it would be wrong to subtract the contribution from the resolved sources from the XRB observations when looking for the DM decay signal. The form of the XRB spectrum with sources subtracted is, in fact, unknown, and the assumption that it has the shape of the initial spectrum, scaled down according to the resolved fraction (as in Abazajian et al. 2001), requires additional justification.

(iii) We find that a more elaborate analysis of the data enables us to put tighter limits on the allowed region of the parameter space  $(m_s, \Omega_s \sin^2 2\theta)$  from the XRB observations. The idea is that the cosmological DM decay spectrum is characterized not only by the total flux but also by a characteristic shape. Being present in the XRB spectrum, it would produce a local feature with some clear maximum and a width greater than the spectral resolution of the instrument. Features of such a scale are clearly absent in the data (smaller features could be present in the spectrum as a result of, for example, element lines, but they cannot produce a bump wider than the spectral resolution). Therefore, one can find that the addition to the standard broad continuum model of the XRB of the DM decay component in the wrong place results in a decrease of the overall quality of the fit of the data with such a two-component model (i.e. an increase in the  $\chi^2$  of the fit). The condition that the two-component model provides an acceptable fit to the data imposes an upper limit on the flux in the DM decay component that is much more restrictive than the limit following from the condition that the flux of the DM component should not exceed the flux in the continuum component.

The paper is organized as follows. In Section 2 we compute the contribution of the radiative decay of sterile neutrinos to the diffuse XRB and compare its shape with that of the measured XRB. We discuss the effects of the non-uniformness of the DM distribution in Section 2.1. In Section 3 we obtain a model-independent exclusion region from *HEAO-1* and *XMM-Newton* observations.

## 2 THE CONTRIBUTION OF DM DECAYS TO THE XRB

A sterile neutrino with a decay width  $\Gamma$  and mass  $m_s$  decays into an active neutrino and emits photons with a line-like spectrum at the energy  $E_\gamma = m_s/2$ . However, photons emitted at different cosmological distances are redshifted on their way to the Earth, so that as a result the photon spectrum is given by

$$\frac{d^2 N}{d\Omega dE} = \frac{\Gamma n_{\text{DM}}^0}{4\pi} \frac{1}{EH(m_s/(2E) - 1)} \quad (1)$$

<sup>1</sup>For example, if the coupling of sterile neutrinos to inflatons is large enough, the main production mechanism will be the creation of sterile neutrinos in inflaton oscillations rather than active–sterile neutrino transition.

(see Masso & Toldra 1999; Abazajian et al. 2001). Here,  $n_{\text{DM}}^0$  is the DM number density at the present time, and  $H(z)$  is the Hubble parameter as a function of redshift. The explicit form of  $H(z)$  depends on the cosmological parameters. This means that the expected dark matter decay spectrum is different for different cosmologies. We are interested in  $z$  corresponding to the epoch more recent than the radiation-dominated Universe, and, therefore,  $H(z)$  can be written as

$$H(z) \simeq H_0 \sqrt{\Omega_\Lambda + \Omega_{\text{matter}}(1+z)^3}, \quad (2)$$

where  $H_0$  is the present-day value of the Hubble parameter and  $\Omega_\Lambda$ ,  $\Omega_{\text{matter}}$  are the cosmological constant and matter contributions to the density of the Universe. Substituting (2) into (1), we find that for small  $z$  the spectrum is approximated as

$$\frac{d^2 N}{d\Omega dE} \simeq \frac{\Gamma n_{\text{DM}}^0}{2\pi H_0} \frac{(2E)^{1/2}}{\sqrt{8E^3 \Omega_\Lambda + \Omega_{\text{matter}} m_s^3}}. \quad (3)$$

Assuming the Majorana nature of neutrino mass, the decay width  $\Gamma$  is related to  $\sin 2\theta$  via (Pal & Wolfenstein 1982; Barger, Phillips & Sarkar 1995)

$$\Gamma = \frac{9\alpha G_F^2}{256 \times 4\pi^4} \sin^2(2\theta) m_s^5 = 5.6 \times 10^{-22} \sin^2 \theta \left( \frac{m_s}{1 \text{ keV}} \right)^5 \text{ s}^{-1}, \quad (4)$$

where  $G_F$  is the Fermi constant.

As an example, we show in Fig. 1 the expected dark matter decay spectrum for the cosmological ‘concordance’ model with  $\Omega_\Lambda \simeq 0.7$ ,  $\Omega_{\text{matter}} \simeq 0.3$ . One can see that close to the maximum the spectrum is roughly a power law with photon index equal to 1 ( $dN/dE \sim E^{-1}$ ).

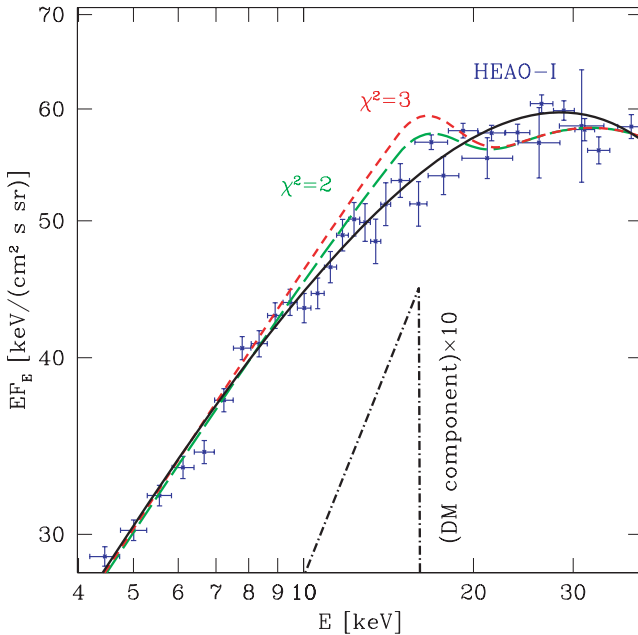


**Figure 1.** Diffuse X-ray background spectrum from the *HEAO-I* mission. The black solid curve shows the empirical fit equation (5) by Gruber et al. (1999). The reduced  $\chi^2$  of this fit is 1.2. Dashed (green and red) lines represent the result of the fit of the same data to a model of the form (5) with an added DM component. The DM decay component (dot-dashed curve) is calculated for the ‘concordance’ model  $\Omega_\Lambda = 0.7$ ,  $\Omega_{\text{matter}} = 0.3$  and for  $m_s = 36.5$  keV. The green (long-dashed) line represents a fit of DM with the mixing angle  $\sin^2 2\theta = 1.9 \times 10^{-12}$ , and the best achievable fit has the reduced  $\chi^2 = 2$ . For the red (short-dashed) line, the mixing angle is  $\sin^2 2\theta = 2.4 \times 10^{-13}$  and the reduced  $\chi^2 = 3$ , which we choose as a border line for the allowed quality of fit.

The measurements of the diffuse XRB (Marshall et al. 1980; Gruber et al. 1999) show that for  $3 \lesssim E \lesssim 60$  keV its form is well approximated by the following analytical expression:

$$\frac{d^2 F_{\text{XRB}}}{dE d\Omega} = C_{\text{XRB}} \exp\left(-\frac{E}{T_{\text{XRB}}}\right) \left[\frac{E}{60 \text{ keV}}\right]^{-\Gamma_{\text{XRB}}+1} \frac{\text{keV}}{\text{keV sr s cm}^2}, \quad (5)$$

where  $C_{\text{XRB}}$  is a normalization constant. In Fig. 1 we show the *HEAO-I* data points<sup>2</sup> together with the above analytical fit (solid black line). Such a form of the XRB spectrum can be explained by active galactic nucleus (AGN) emission, under certain assumptions about AGN populations (Worsley et al. 2005; Treister & Urry 2005). Below  $\sim 15$  keV, the XRB was measured by many X-ray missions and the background was found to follow a power law with photon index  $\Gamma_{\text{XRB}} \simeq 1.3\text{--}1.4$  (Gruber et al. 1999; Lumb et al. 2002; Revnivtsev et al. 2003; Revnivtsev et al. 2005; Gilli 2003; Barger 2003). The analysis of Gruber et al. (1999) finds  $T_{\text{XRB}} = 41.13$  keV and  $C_{\text{XRB}} = 7.9$ . The DM decay component produces a harder spectrum, as can be seen from Fig. 1.

## 2.1 The uniformness of the DM density in the Universe

Most of the power in the very hard DM decay spectrum of Fig. 1 is emitted in the narrow energy interval close to the maximal energy  $E_{\text{max}} \simeq m_s/2$ . From equation (3) it can be seen that emission in this energy range is produced by neutrinos decaying at the present epoch ( $z \simeq 0$ ). For the case of the ‘concordance’ model, the DM decay spectrum is characterized by the very hard inverted power law  $dN/dE \sim E^{1/2}$  below an energy of  $\sim E_{\text{max}}/2$ . The energy flux drops by an order of magnitude at energies  $\sim E_{\text{max}}/4$ , which correspond to the redshift  $z \simeq 3$ . Thus, most of the DM decay signal is collected from low redshifts.

It is known that the process of structure formation leads to significant clustering of the dark matter at small redshifts. The signal from DM decays at small  $z$  is thus dominated by the sum of contributions from the point-like sources corresponding to large DM concentrations, such as galaxies or clusters of galaxies.

Abazajian et al. (2001) and Mapelli & Ferrara (2005) argued that the clustering of the DM at small redshifts makes it difficult for the instruments that measure the diffuse XRB to detect the signal from the DM decays at small redshifts. Indeed, measurements of the diffuse XRB carried out with narrow-field instruments, such as *Chandra* or *XMM-Newton*, can miss the DM signal because of the absence of large nearby galaxies or clusters of galaxies in the fields used for the deep observations and background measurements. As a measure for galaxy clustering, one can take the distribution of the number of galaxies as a function of the distance ( $N_{\text{gal}}(r)$ ). The Sloan Digital Sky Survey data show that the function  $\langle N_{\text{gal}}(r) \rangle$  becomes constant for  $r \gtrsim 100$  Mpc (which corresponds to a redshift  $z \sim 0.02$ ) (see, for example, Joyce et al. 2005). Therefore, an instrument with a field of view (FoV) that encompasses a volume  $\sim (100 \text{ Mpc})^3$  at distances corresponding to  $z \lesssim 1$  will observe a homogeneous matter distribution. Let us take the Hubble distance as an estimate for such distances:  $H_0^{-1} \sim 3.8 \times 10^3$  Mpc (here,  $H_0$  is the present-day Hubble constant). Then, the minimal FoV  $\theta_{\text{fov}}$  is determined from a simple relationship,  $\theta_{\text{fov}}^2 H_0^{-3} \gtrsim (100 \text{ Mpc})^3$ , i.e.  $\theta_{\text{fov}} \gtrsim 15'$ . The FoV of *XMM-Newton* is precisely of this order, namely  $\theta_{\text{xmm}} \sim 30'$ . Therefore, the strongest signal from small  $z$  can be missed if only ‘empty fields’ are selected for the *XMM-Newton* XRB observations.

<sup>2</sup>We thank D. Gruber for sharing these data with us and for many useful comments.

On the other hand, wide FoV instruments or the instruments that have conducted all-sky surveys, such as *HEAO-1* or *ROSAT*, cannot miss the largest contribution to the DM decay signal from  $z < 10$  because of the full sky coverage. Thus, the above argument should be used in a reverse sense: to find the DM decay signal it is necessary to use the data on the XRB collected from the whole sky, rather than from the ‘deep field’ observations of a narrow-field instrument.

### 3 RESTRICTIONS ON PARAMETERS OF STERILE NEUTRINOS FROM MEASUREMENTS OF THE DIFFUSE X-RAY BACKGROUND

#### 3.1 Restrictions from *HEAO-1* measurements

The above analytical approximation (5) provides a good fit to the *HEAO-1* data. No DM decay feature with a spectrum of the form of (3) (corrected for the spectral resolution of the instrument) is evident in the data. A straightforward constraint on the possible contribution of DM decays to the XRB spectrum is that the flux of the DM decay contribution does not exceed the total flux. Such an approach was used by Dolgov & Hansen (2002), who applied it to the broad-band XRB model of Ressel & Turner (1989). Using the fit (5) of Gruber et al. (1999), which gives a much better description in the kilo-electronvolt region, we obtain an exclusion curve, shown as the green dot-dashed line in Fig. 2.

Clearly this restriction is model-independent and rigorous. However, it can be made stronger. Indeed, the experimentally measured XRB is monotonic at energies from kilo-electronvolts to giga-electronvolts (see Gruber et al. 1999). If the flux of the DM had

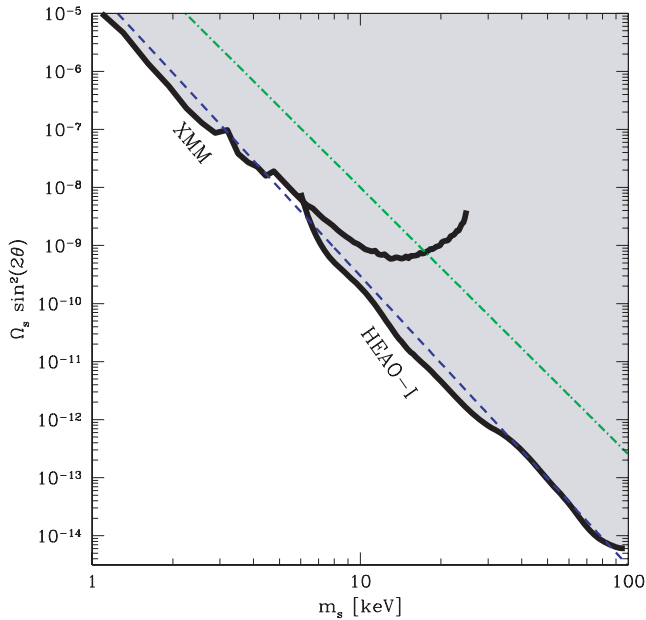


**Figure 2.** Exclusion plot on parameters  $m_s$  and  $\sin^2 2\theta$  using *HEAO-1* and *XMM-Newton* data. The values in the non-shaded region are allowed. In the region where both *HEAO-1* and *XMM-Newton* data are available, *HEAO-1* provides a more stringent constraint (as discussed in Section 3.2). We assumed that sterile neutrinos constitute 100 per cent of all the DM (i.e.  $\Omega_s = \Omega_{\text{DM}}$ ). To remove dependence on the value of  $\Omega_{\text{DM}}$ , we choose to plot  $\Omega_s \sin^2 2\theta$  rather than  $\sin^2 2\theta$ . The results can be described by a simple empirical formula, equation (6) (thin blue dashed line). The dot-dashed green line represents the exclusion region obtained if all 100 per cent of the XRB flux is attributed to DM at energies  $E \lesssim m_s/2$ .

contributed a significant part to the total XRB, contributions to the XRB *unrelated* to the radiative DM decay should combine into a spectrum with a sudden narrow ‘dip’. In particular, at energies  $E \geq m_s/2$  some new physical phenomena should have suddenly ‘kicked in’, causing the spectrum to experience a very sharp ‘jump’. Moreover, the form of this dip must have been almost the same as the DM contribution with a minus sign. This would have required a mechanism for a very precise fine-tuning of contributions to the XRB between the DM and various physical phenomena, or simply a chance coincidence. Of course, such a conspiracy cannot be absolutely excluded, in particular because of the lack of unambiguous theoretical predictions of the shape of the XRB spectrum. However, it is very unlikely that there would be a precise cancellation of contributions of a different nature. Therefore, in what follows we will assume that such a situation does not occur (in particular, this does not occur in models attributing the existing XRB shape to AGN emissions: Worsley et al. 2005; Treister & Urry 2005).

In the present work we therefore argue that the constraint on the possible DM contribution to the XRB resulting from *HEAO-1* data can be improved using a statistical analysis of the data. Our strategy will be the following. We take the actual *HEAO-1* data and fit them to a model of the form (5) (varying  $C_{\text{XRB}}, T_{\text{XRB}}, \Gamma_{\text{XRB}}$  plus an additional DM flux (3) (corrected for the spectral resolution of *HEAO-1* instruments). The addition of a large DM contribution would worsen the quality of the model fit to the data, while the addition of a small DM contribution does not change the overall fit quality. Thus, one can put a restriction on the DM contribution by allowing the DM component to worsen the fit by a certain value. Taking into account that we have around 40 degrees of freedom of the system under consideration, we take the maximal allowed value of the reduced chi-square of the fit to be  $\chi^2 < 3$ . Thus on a technical level our method restricts the flux of DM to be of the order of errors of measured XRB flux, rather than its total value.

The results of the application of the above algorithm to the data are shown in Fig. 2. The allowed values of  $(m_s, \Omega_s \sin^2 2\theta)$  are those in the unshaded region.<sup>3</sup> The shaded region below the dot-dashed line is excluded under the assumption that the XRB spectrum does not have an unknown feature (a ‘dip’) fine-tuned to be located precisely at energies at which DM contributes.

According to equations (3) and (4), the flux of DM is proportional to  $\Omega_s \sin^2 2\theta$ . We therefore choose to plot this value rather than the conventional  $\sin^2 2\theta$  on the y-axis of Fig. 2. This removes uncertainty, related to the determination of  $\Omega_{\text{DM}}$ . Notice that the results obtained from *HEAO-1* data (thick solid lines in Fig. 2) are model-independent and can be applied to any DM candidate that has a decay channel into a lighter particle and a photon, with its decay width  $\Gamma$  related to  $\sin \theta$  via equation (4).

#### 3.2 Restriction from *XMM-Newton* background measurements

In the energy band below 10 keV the XRB has been studied by numerous narrow-FoV instruments, including *XMM-Newton*. The increased angular resolution and sensitivity of these instruments

<sup>3</sup>The normalization of the XRB spectrum, measured by *HEAO-1*, is known to be lower than any other XRB measurements (Gilli 2003; Moretti et al. 2003). In Fig. 2, therefore, *HEAO-1* data were *increased* by 40 per cent according to De Luca & Molendi (2005), Worsley et al. (2005) and Treister & Urry (2005) (see, however, Gilli 2003). This weakens the restriction of Fig. 2 by about 10 per cent, as compared with actual *HEAO-1* data.

has enabled some 90 per cent of the XRB to be resolved into point sources (Brandt & Hasinger 2005; De Luca & Molendi 2005; Bauer et al. 2004). In theory, better sensitivity should enable us to put tighter constraints on the possible DM contribution to the XRB. However, in this section we show that this is not the case.

The key point that leads to such a conclusion is that the better sensitivity (to point sources) of these instruments is achieved as a result of the better angular resolution, rather than as a result of the increase of the effective collection area. Thus, if one is interested in the diffuse sources, the sensitivity is not improved compared with *HEAO-1*. On the contrary, in the narrow-FoV instruments the XRB signal is collected from a smaller portion of the sky, which leads to lower statistics of the signal. At the same time, the instrumental background (which is thought to arise from cosmic rays hitting the instrument) is roughly the same for narrow- and wide-field instruments. Thus, the ratio of the counts arising from the photons of the XRB to the instrumental background counts is smaller for the narrow-field instruments, and one needs larger integration times to achieve good statistical significance of the XRB signal.

The above problem would not affect the constraints on  $m_s, \sin \theta$  if they were imposed by the condition for the flux in the DM decay component not to exceed the total XRB flux in a given energy interval. However, as the statistical significance of the XRB signal in the narrow-FoV instruments is lower, bigger errors decrease the  $\chi^2$ -value, and therefore the imposed limit on DM will be worse than that of the corresponding wide-FoV instruments.

The exclusion plot in the  $(m_s, \Omega_s \sin^2 2\theta)$  parameter space obtained from the analysis of the *XMM-Newton* data is shown in Fig. 2. We took the actual data of two collections of *XMM-Newton* background observations (Lumb et al. 2002), total exposure time  $\sim 450$  ks; and Read & Ponman (2003), total observation time  $\sim 1$  Ms. The form of the *XMM-Newton* background is fitted by a power law with index  $\Gamma = 1.4$  (Lumb et al. 2002)), in agreement with equation (5). Applying our method to *XMM-Newton* data, as described in the previous section, we find the restrictions shown in Fig. 2. In the neutrino mass region  $6 \lesssim m_s \lesssim 20$  keV, where both *HEAO-1* and *XMM-Newton* data are available, the *XMM-Newton* background provides a weaker restriction than the data from *HEAO-1*, because of the reason discussed above (the *XMM-Newton* FoV has a radius of 15 arcmin, which is much smaller than that of the *HEAO-1*, namely  $\sim 3^\circ$  for A2 HED detectors). In the case of *XMM-Newton*, the statistical error at energies above roughly 7 keV is dominated by instrumental background, while in the case of *HEAO-1* the errors at these energies are dominated by the diffuse XRB. As a result, errors of flux determination are smaller for *HEAO-1* data, thus providing more stringent restrictions. Of course, the *XMM-Newton* data provide constraints on the parameters of the neutrino in the region  $1 \lesssim m_s \lesssim 6$  keV, where *HEAO-1* data are not available. The data in Fig. 2 fit to the simple empirical formula

$$\Omega_s \sin^2(2\theta) < 3 \times 10^{-5} \left( \frac{m_s}{\text{keV}} \right)^{-5}. \quad (6)$$

### 3.3 Discussion

In this work we have looked for signatures of sterile neutrino decay in the extragalactic XRB. The main result of our paper is the plot in Fig. 2, which constrains the properties of sterile neutrinos as dark matter candidates.

Let us compare our exclusion plot with similar plots found in other works. Dolgov & Hansen (2002) used a broad-band limit, put on the XRB by Ressel & Turner (1989), to find restrictions on sterile

neutrino parameters. First of all, in the kilo-electronvolt energy band the limit of Ressel & Turner (1989) is weaker than that of Gruber et al. (1999), which we use in this paper. Therefore the dot-dashed line in Fig. 2 provides model-independent restrictions on the parameters of sterile neutrinos that are stronger than the similar bound in fig. 4 of Dolgov & Hansen (2002). Second, as discussed in Section 3, we put a restriction on the parameters of sterile neutrinos based on the statistical analysis of the actual experimental data of *HEAO-1* and *XMM-Newton* missions. Such a constraint is possible under the assumption that there is no extremely unlikely fine-tuning between various components contributing to the XRB. In other words, the observed XRB spectrum is monotonic in the kilo-electronvolt range (at energies below  $\sim 15$  keV this was checked by various X-ray missions, including recent measurements by *XMM-Newton* and *Chandra*). Therefore, we assume that the XRB spectrum *without* DM has no ‘dip’ and exactly matches the shape and location of the DM contribution. The results of our analysis are shown in the thick black solid line in Fig. 2. As the statistical quality of the data is good, this gives about two orders of magnitude stronger restrictions than those represented by the dot-dashed line. The region between the solid (or its empirical fit, equation 6) and dot-dashed lines is excluded under the assumptions discussed above.

Abazajian et al. (2001) provide an exclusion plot (also quoted by Abazajian 2006) based on observations of the Virgo cluster. Boyarsky et al. (2006) show that the restrictions from clusters of galaxies are weaker than those of Abazajian (2006); however, in the mass range  $2 \text{ keV} \lesssim m_s \lesssim 10 \text{ keV}$  they are 2 to 4 times better than those coming from the XRB. For a detailed comparison of our results with those of Abazajian (2006), see Boyarsky et al. (2006).

In some cases, such as in the Dodelson–Widrow (DW) scenario, (Dodelson & Widrow 1993)<sup>4</sup> there exists a relationship between the mass of a sterile neutrino, the mixing angle and the present-day sterile neutrino density  $\Omega_s$  (Dolgov & Hansen 2002; Abazajian et al. 2001; Abazajian 2006). Because both the sterile neutrino abundance and the gamma-ray flux depend on the mixing angle  $\theta$  and the sterile neutrino mass  $m_s$  only, this provides an upper limit on the sterile neutrino mass in the DW scenario. According to the computation of sterile neutrino abundance made in Abazajian (2006), the corresponding limit following from the X-ray bound found in the present paper reads  $m_s < 8.9 \text{ keV}$  for the DW sterile neutrino. However, even in the DW scenario this number is subject to uncertainties that are difficult to estimate, because the peak of the sterile neutrino production falls into the range of temperatures where neither a hadronic nor a quark description of the hot plasma is possible.

The Standard Model augmented by just one sterile neutrino cannot explain the neutrino oscillation data, and thus extra ingredients should be added to it. The analysis of Asaka, Kusenko & Shaposhnikov (2006) shows that, in a more realistic model, the  $\nu$ MSM, the relationship between the mass of the sterile neutrino, the mixing angle and the present-day sterile neutrino density  $\Omega_s$  changes, depending on unknown parameters, such as the masses and couplings of extra particles and primordial abundances of sterile neutrinos. Therefore, for a general case one cannot put a model-independent restriction on the mass of the sterile neutrino  $m_s$ , and

<sup>4</sup>In this scenario it is assumed that there is just one species of sterile neutrino, that their concentration was zero at temperatures higher than 1 GeV, that there were no substantial lepton asymmetries, and that the Universe reheating temperature was larger than 1 GeV.

the search for a narrow line coming from its decays should be carried out in all energy ranges.

The results of this work show that a possible strategy to look for a feature of DM decay in the XRB is to use data from ‘all-sky surveys’ rather than ‘deep-field observations’, and to utilize instruments with the largest possible FoV (rather than the best angular/spectral resolution). An example of such an instrument is *INTEGRAL*, with which observations of the XRB are currently planned.

## ACKNOWLEDGMENTS

We would like to acknowledge useful discussions with K. Abazajian, A. Kusenko, I. Tkachev and R. Rosner. This work was supported in part by the Swiss Science Foundation and by European Research Training Network contract 005104 ‘ForcesUniverse’. OR was supported by a Marie Curie International Fellowship within the 6th European Community Framework Programme.

## REFERENCES

- Abazajian K., 2006, *Phys. Rev. D*, 73, 063506  
 Abazajian K., Fuller G. M., Tucker W. H., 2001, *ApJ*, 562, 593  
 Ahmad Q. R. et al., 2002, *Phys. Rev. Lett.*, 89, 011301  
 Asaka T., Shaposhnikov M., 2005 *Phys. Lett. B*, 620, 17  
 Asaka T., Blanchet S., Shaposhnikov M., 2005, *Phys. Lett. B*, 631, 151  
 Asaka T., Kusenko A., Shaposhnikov M., 2006, *hep-ph/0602150*  
 Barger A. J., 2003, *Rev. Mex. AA Ser. Conf.*, 17, 226  
 Barger V. D., Phillips R. J. N., Sarkar S., 1995, *Phys. Lett. B*, 352, 365; Erratum, *ibid.*, 356, 617  
 Barkovich M., D’Olivo J. C., Montemayor R., 2004, *Phys. Rev. D*, 70, 043005  
 Bauer F. E., Alexander D. M., Brandt W. N., Schneider D. P., Treister E., Hornschemeier A. E., Garmire G. P., 2004, *AJ*, 128, 2048  
 Boyarsky A., Neronov A., Ruchayskiy O., Shaposhnikov M., 2006, *astro-ph/0603368*  
 Brandt W. N., Hasinger G., 2005, *ARA&A*, 43, 827  
 De Luca A., Molendi S., 2004, *A&A*, 419, 837  
 Dodelson S., Widrow L. M., 1993, *Phys. Rev. Lett.*, 72, 17  
 Dolgov A. D., Hansen S. H., 2002, *Astropart. Phys.*, 16, 339  
 Eguchi K. et al., 2003, *Phys. Rev. Lett.*, 90, 021802  
 Fryer C. L., Kusenko A., 2006, *ApJS*, 163, 335  
 Fukugita M., Yanagida T., 1986, *Phys. Lett. B*, 174, 45  
 Fukuda Y. et al., 1998, *Phys. Rev. Lett.*, 81, 1562  
 Fuller G. M., Kusenko A., Mocioiu I., Pascoli S., 2003, *Phys. Rev. D*, 68, 103002  
 Gell-Mann M., Ramond P., Slansky R., 1980, in van Nieuwenhuizen P., Freedman D. Z., eds, *Supergravity*. North Holland, Amsterdam  
 Gilli R., 2003, in Done C., Puchnarewicz E. M., Ward M. J., eds, *New X-ray Results from Clusters of Galaxies and Black Holes*. Invited talk, in press (*astro-ph/0303115*)  
 Glashow S. L., 1979, in Levy M. et al., eds, *Proc. Cargèse Summer Institute on Quarks and Leptons*. Plenum, New York, p. 707  
 Gruber D. E., Matteson J. L., Peterson L. E., Jung G. V., 1999, *ApJ*, 520, 124  
 Hansen S. H., Lesgourgues J., Pastor S., Silk J., 2002, *MNRAS*, 333, 544  
 Joyce M., Sylos Labini F., Gabrielli A., Montuori M., Pietronero L., 2005, *A&A*, 443, 11  
 Kusenko A., Segre G., 1997, *Phys. Lett. B*, 396, 197  
 Kuzmin V. A., Rubakov V. A., Shaposhnikov M. E., 1985, *Phys. Lett. B*, 155, 36  
 Lumb D. H., Warwick R. S., Page M., De Luca A., 2002, *A&A*, 389, 93  
 Mapelli M., Ferrara A., 2005, *MNRAS*, 364, 2  
 Marshall F., Boldt E. A., Holt S. S., Miller R. B., Mushotzky R. E., Rose L. A., Rothschild R. E., Serlemitsos R. J., 1980, *ApJ*, 235, 4  
 Mastro E., Toldra R., 1999, *Phys. Rev. D*, 60, 083503  
 Minkowski P., 1977, *Phys. Lett. B*, 67, 421  
 Mohapatra R. N., Senjanovic G., 1980, *Phys. Rev. Lett.*, 44, 912  
 Moretti A., Campana S., Lazzati D., Tagliaferri G., 2003, *ApJ*, 588, 696  
 Pal P. B., Wolfenstein L., 1982, *Phys. Rev. D*, 25, 766  
 Ramond P., 1979, Talk given at the Sanibel Symposium, preprint CALT-68-709 (retroprinted as *hep-ph/9809459*)  
 Read A. M., Ponman T. J., 2003, *A&A*, 409, 395  
 Ressel M. T., Turner M. S., 1989, *Comments Astrophys.*, 14, 323  
 Revnivtsev M., Gilfanov M., Sunyaev R., Jahoda K., Markwardt C., 2003, *A&A*, 411, 329  
 Revnivtsev M., Gilfanov M., Jahoda K., Sunyaev K., 2005, *A&A*, 444, 381  
 Treister E., Urry C. M., 2005, *ApJ*, 630, 115  
 Viel M., Lesgourgues J., Haehnelt M. G., Matarrese S., Riotto A., 2005, *Phys. Rev. D*, 71, 063534  
 Worsley M. A. et al., 2005, *MNRAS*, 357, 1281

This paper has been typeset from a  $\text{\LaTeX}$  file prepared by the author.